# Experimental Investigation of the Trailing Edge Noise Mechanism

J. C. Yu*
*NASA Langley Research Center, Hampton, Va.*
and
C. K. W. Tam†
*Flordia State University, Tallahassee, Fla.*

**An experimental investigation has been conducted to understand the physical mechanism of noise generation from a turbulent wall jet discharging over a flat plate and interacting with its sharp trailing edge. An aspect ratio 10 rectangular nozzle was used to provide the wall jet. Measurements made consist of far-field noise, surface pressure fluctuations, turbulent velocity fluctuations, and two-point space-time cross correlations among these quantities. The results strongly suggest that the generation mechanism is the interaction of the convecting large-scale quasiorderly disturbance in the upper free shear layer of the wall jet with the trailing edge. The interaction also excites large-scale strong vortical motion in the trailing edge wake. The dominant part of the sound field is highly coherent and in phase opposition across the trailing edge.**

## Introduction

THE interaction between turbulent flow leaving the surface of a rigid body and the trailing edge is generally recognized as an important noise source in at least two classes of aeroacoustic problems. One class involves turbulent jet flow discharging over a rigid surface of finite extent,[1] examples of which are the upper surface blown flap and the externally blown flap. The other class involves an airfoil placed in a uniform stream.[2,3] This paper addresses itself to the trailing edge noise generation in the first class of problem.

Analytical efforts made in the past on this subject were invariably based on some hypothesized physical model of the source mechanism. Powell[4] considered the turbulence within the wall-boundary layer upstream of the edge as the source. Ffowcs Williams and Hall[5] investigated the role of the edge in scattering of the sound field produced by quadrupoles in close proximity to the edge. Hayden[6] modeled the trailing edge noise source as a localizdd dipole at the edge. Chase,[7,8] Chandiramani,[9] and Amiet[10] analyzed the noise radiation produced as a result of the scattering of the hydrodynamic pressure wave by the trailing edge. By adding certain assumptions to the analysis, each theory is capable of predicting the directivity, total power, and power spectrum function of the trailing edge noise based on measurable flow parameters. In fact, the predicted trends, with minor variations, are fairly consistent among the different theories. These theoretical trends have also been partially confirmed by far-field noise measurements obtained with blown flap type of flowfields. An extensive review of the theoretical efforts on trailing edge noise production has been given recently by Howe.[11] A unified theory of trailing edge noise was also proposed by the same author.

In spite of the agreement between analytical predictions and far-field measurements, the basic physical process by which a trailing edge generates sound remains to be understood. The required source information has to be obtained from a detailed knowledge of the fluctuating flows. It is only over recent years that some limited studies of the fluctuating fields near the trailing edge have been reported.[12-14]

Upon recognizing the need for an in-depth experimental investigation of both the fluctuating flowfield and the radiated far-field in order to provide a better understanding of the precise physical mechanism by which a trailing edge generates noise, the authors initiated an experimental program to examine both the fluctuating flowfield and the radiated noise for a turbulent wall jet over a flat plate of finite chord.[15]

Preliminary experimental findings revealed that for flow conditions of practical interest, large-scale quasiorderly structures exist in the outer shear layer of the wall jet and downstream of the trailing edge. These observed structures resemble the two-dimensional flow instability observed by Davey and Roshko[16] and also the large-scale structure in the work of Brown and Roshko.[17] This observation has suggested to us that the physical mechanism of trailing edge noise may be intimately related to the interaction between the large-scale flow structures and the trailing edge.

The present paper presents some highlights of the experimental investigation of the fluctuating surface pressure, turbulent velocity fluctuations, and far-field noise. To reveal the role that the observed large structures play in noise generation, the discussion will center on the statistical interdependence among the velocity fluctuations, surface-pressure fluctuations, and far-field noise deduced from two-point space-time cross correlations. Certain redundancy was purposely built into the experiment so that more than one piece of evidence could be used to reach a definitive conclusion.

## Experimental Apparatus, Instrumentation, and Procedures

Both acoustic measurements and flow measurements reported here were made in the Anechoic Flow Facility of the Acoustics and Noise Reduction Division, NASA Langley Research Center. The nozzle used to generate the jet flow had an overall contraction ratio of 520. The exit area is 15 cm $\times$ 1.5 cm, thus providing an aspect ratio of 10. The flat plate used in conjunction with the nozzle to provide the wall jet had a chord length $L = 8.5$ times the nozzle height $H$ and a span of 0.61 m. The trailing edge of the plate was machined to a knife-edge. A schematic showing the nozzle and plate arrangement is illustrated in Fig. 1. The nozzle was operated

Presented as Paper 77-1291 at the AIAA 4th Aeroacoustics Conference, Atlanta, Ga., Oct. 3-5, 1977; submitted Feb. 2, 1978; revision received June 12, 1978. 

Index categories: Aeroacoustics; Nonsteady Aerodynamics; Jets, Wakes, and Viscid-Inviscid Flow Interactions.

*Aero-Space Technologist. Member AIAA.
†Professor, Dept. of Mathematics. Member AIAA.

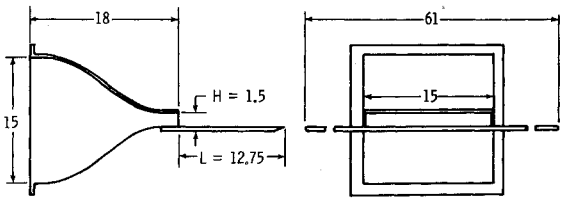


**Fig. 1 Schematic of nozzle and plate arrangement (all dimensions in centimeters).**

at a nominal exit velocity $U_J$ of 152 m/s which gives a Reynolds number based on nozzle height of $1.54 \times 10^5$. The boundary layer at the nozzle exit was very thin and the exit turbulence level was about 0.2%. The core length of the wall jet was about 11 nozzle heights.

The instrumentation used in the correlation analysis consists of seven surface pressure channels, two far-field acoustic pressure channels, and two hot-wire channels. The surface pressure fluctuations along the central chord of the plate were monitored by ⅛-in. B&K condenser microphones flush mounted to the flow side of the plate and ¼-in. B&K free-field microphones were used to measure the radiated sound in a plane perpendicular to and bisecting the plate. A DISA 55A38 miniature crosswire probe was used with TSI constant temperature anemometers and linearizers. A sketch showing the transducer arrangment is given in Fig. 2.

In view of the extensive correlation analysis planned, the phase response characteristics among different data channels must be known to insure the validity of analysis. The phase response of all microphone channels was calibrated over the bandwidth of measurement from 100 Hz to 10 kHz. The seven surface microphone channels were matched in phase to within 1 deg over the bandwidth of measurement. The two far-field microphone channels were phase matched within 2 deg over the same bandwidth. Between surface microphone and far-field microphones, the phase match was within 5 deg up to 2 kHz.

Phase calibration between hot-wire channels and microphones was not established directly. However, an estimate of the possible phase mismatch between hot wires and microphones was made based on the shock-tube calibration results reported by Lau et al.[18] It was estimated that the phase mismatch between the hot wire and microphones used in the present study should be less than 20 deg up to 3 kHz. Since, the major frequency of interest in this study is around 1 kHz, the mismatch was considered acceptable.

To rule out the possibility of contaminations of sound field and fluctuating surface-pressure field by the introduction of hot-wire probe, spectra were obtained for all microphone channels with and without the hot wire in the flow. This was done for a number of wire locations. It was found that the surface-pressure spectrum was repeatable within 0.5 dB and the far-field noise spectrum repeatable within 1 dB.

Additional details on instrumentation and procedures may be found in Ref. 19.

## Experimental Results

### Shadowgraph Observations

Typical spark shadowgraphs of the flowfield are reproduced in Figs. 3 and 4. These shadowgraphs clearly indicate the existence of large-scale, quasiorderly flow structure in the upper shear layer (USL) of the wall jet. The observed flow structure originated a short distance downstream of the nozzle exit. The apparent spacing of these quasiorderly disturbances varies between three and four nozzle heights. The vortical structure which appears in the trailing edge wake (TEW) is believed to be the result of a strong interaction between the large-scale disturbance in the USL of the wall jet and the plate trailing edge. This interaction caused the flow downstream of the edge to roll up,

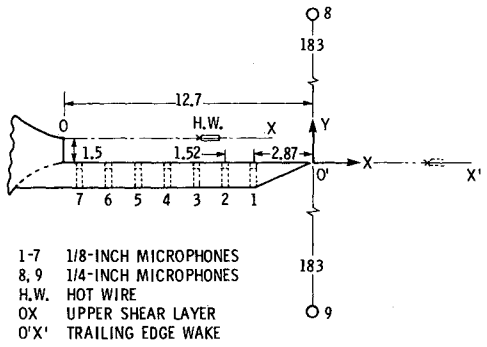


**Fig. 2 Sketch showing transducer arrangement.**

forming a discrete vortex of opposite rotation. In the process of this interaction a fairly coherent sound field is generated. The supporting evidence of these statements will be discussed in subsequent sections.

It is perhaps pertinent to mention that some exploratory shadowgraphic studies were conducted to determine the dependence of the observed large-scale flow structure on the initial conditions. This was done by placing a tripping wire or sandpaper strip on the upper nozzle wall, the lower nozzle wall, and at the trailing edge. No noticeable changes were observed. In fact, these structures were so persistent that they remained even when a sawtooth plate was introduced vertically into the free shear layer at the upper nozzle lip.

### Far-Field Noise and Surface-Pressure Fluctuations

Autospectral density functions of surface pressure fluctuations recorded at microphone 1 (see Fig. 2 for microphone location) and far-field noise at microphone 8 were compared in Fig. 5. Note that both spectra are concentrated within a rather narrow band and that a common spectral peak occurs at about 1300 Hz. The spectrum for microphone 9 is similar to microphone 8. The spectra for other surface microphones (results not shown), however, indicated an evolutionary process in the wall pressure and are thought to reflect the development (growth) of the large-scale disturbance in the upper free shear layer.

The coherence of the sound field is indicated by the normalized cross-correlation function $\rho_{AB}(\tau)$ (hereafter referred to as "correlation") obtained between the microphones 8 and 9 (see Fig. 6). The convention used is

$$\rho_{AB}(\tau) = R_{AB}(\tau) / \sqrt{R_{AA}(0) R_{BB}(0)}$$

where

$$R_{AB}(\tau) = \langle A(\tau) B(t+\tau) \rangle$$

$\tau$ is the time delay and $\langle\ \rangle$ denotes the time average. It can be seen that sound received by the two microphones is highly coherent $|\rho| \simeq 0.8$, in phase opposition, and the maximum correlation occurs at zero time delay. The phase opposition implies that the motion of the source is in phase opposition with respect to the two microphones. Such behavior would also be exhibited if the source of sound had a dipole nature. The maximum correlation at zero time delay may be used to locate the apparent source of sound. The delay window width used in obtaining the correlation shown in Fig. 6 was 10 $\mu$s which corresponds to a spatial resolution of 0.35 cm ($\simeq$ ¼ nozzle height $H$) based on the ambient speed of sound. Thus the occurrence of maximum correlation at zero time delay between two far-field microphones implies that the apparent source of sound is within ¼ nozzle height from the trailing edge.

To quantify the observed large-scale flow disturbances, the scale and convection speed were determined. This was done by cross-correlating the surface pressure field. The spatial correlation using microphone 1 as reference is given in Fig. 7.

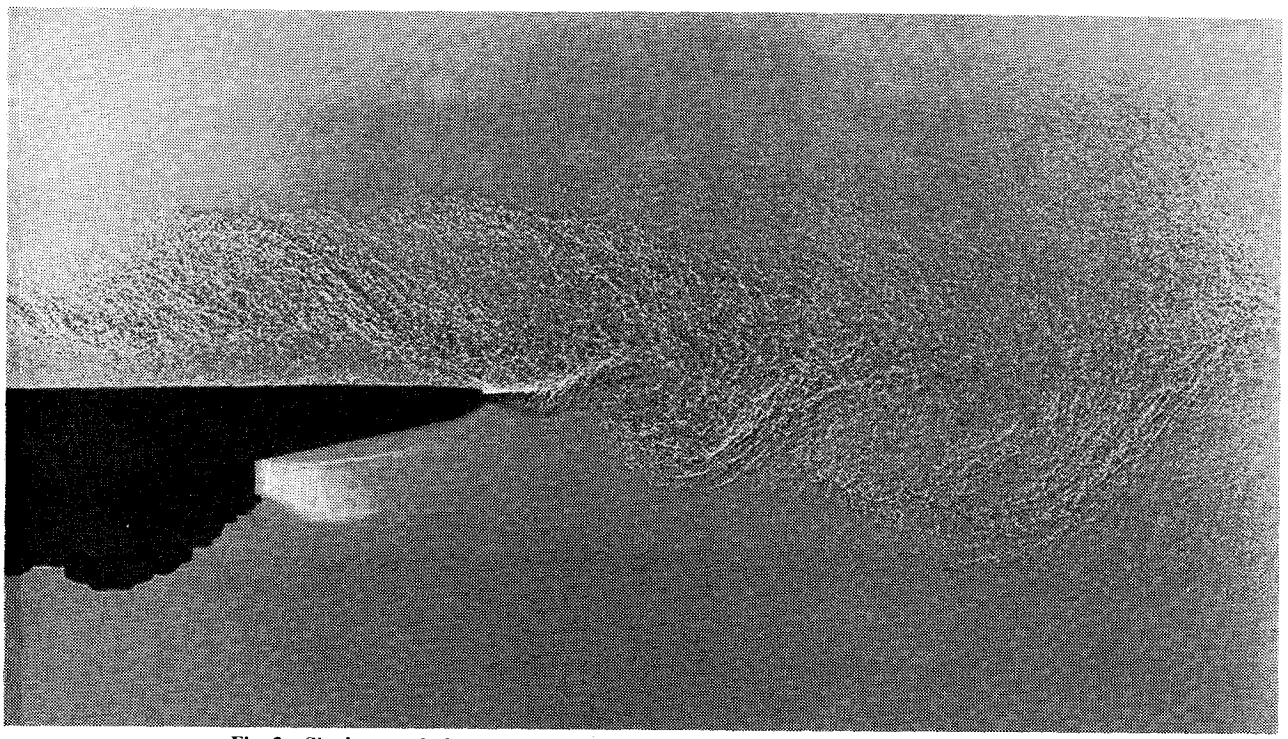

**Fig. 3 Shadowgraph showing flowfield near the trailing edge. $U_j = 194$ m/s, $L/H = 8$.**

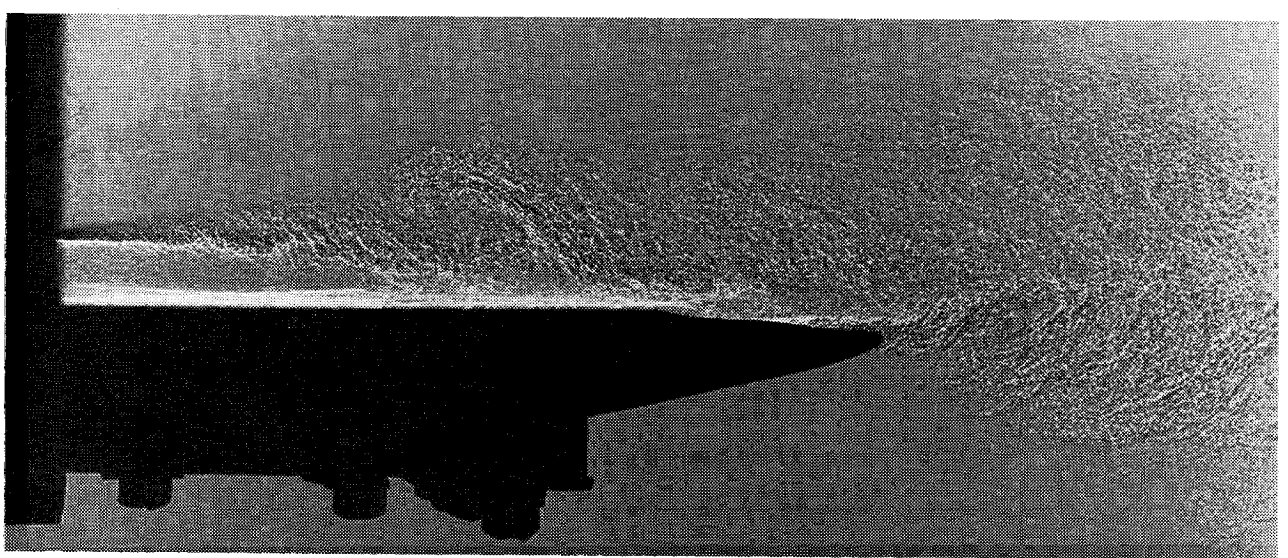

**Fig. 4 Shadowgraph showing flowfield near the nozzle exit. $U_j = 195$ m/s, $L/H = 8$.**

The oscillatory nature of the spatial correlation suggests the existence of the quasiorderly structure. The length scale, or rather the "wavelength," $\lambda$ is about $4H$, which agrees with the spacing of the disturbance deduced directly from shadowgraphs. The envelope of the space-time cross correlations of the surface pressure is shown in Fig. 8. The value of the peak correlation $\rho_{AB}(\tau)$ and the time delay at which the peak occurs are also indicated in the figure. The convection speed $U_c$ of the disturbance indicated by the slope of the spatial separation of the microphones $\xi$ vs the time delay $\tau$ line has a value of $U_c/U_j = 0.6$.

Typical correlations between far-field sound $p$ and surface pressure $p_s$ are shown in Fig. 9. In analyzing these data, the maximum absolute peak of the correlation obtained with microphone 1 was chosen and the variation of the amplitude of this peak and its location in delay time was followed. The results so obtained are plotted in Fig. 10. Note that correlations between microphone 8 and all surface microphones are in exact phase opposition with its counterpart of microphone 9. The magnitude of correlation for both far-field microphones increases monotonically as the plate trailing edge is approached, indicating the importance of the plate trailing edge in sound radiation. The time delay which corresponds to the maximum correlation, however, decreases monotonically as the trailing edge is approached. Moreover, all of the time delays shown on the figure are greater than the acoustic transmission time required between the surface microphone and the far-field microphone. The minimum value of time delay of 5.51 ms is obtained with microphone 1. This value should be compared with the calculated acoustic transmission time (based on ambient speed of sound) which varies from 5.28 ms for microphones 7 to 5.27 ms for microphone 1.

Another interesting feature shown on Fig. 10 is that the $\xi$ vs $\tau$ plot forms a straight line and the slope of it, $(d\xi/d\tau)$, corresponds to a velocity of 0.59 $U_j$ which is very close to the convection speed deduced from surface pressure correlations. This may be explained if it is assumed that the large-scale

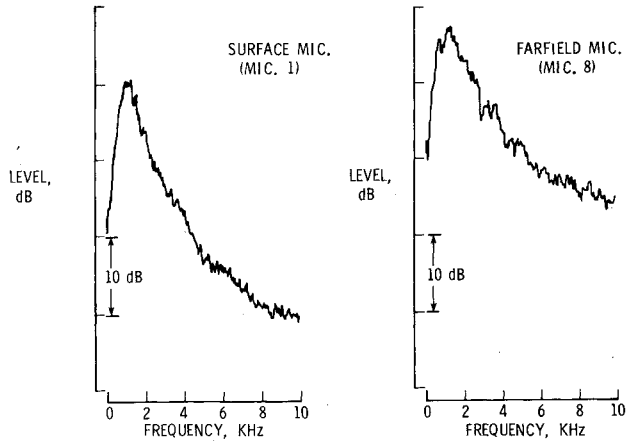


**Fig. 5 Comparison of spectral density functions of surface pressure and far-field noise.**

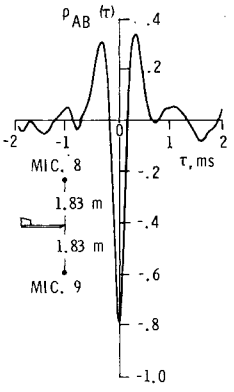


**Fig. 6 Cross-correlation of far-field noise.**

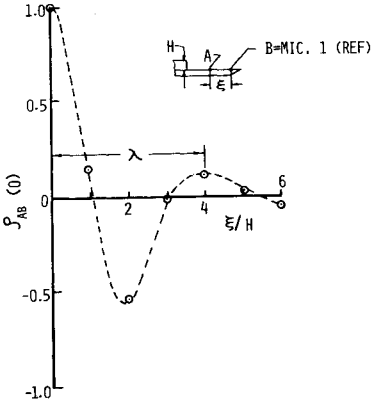


**Fig. 7 Spatial correlation of surface pressure.**

disturbance is being convected rather quietly towards the trailing edge. Upon coming close to the edge, it interacts with the edge and a coherent acoustic radiation results. With this picture in mind, it is easy to see that the peak correlation between surface microphones and far-field microphones should occur at a time delay given by

$$\tau = \frac{\sqrt{r^2 + \xi_0^2}}{C_0} + \frac{\xi - \xi_0}{U_c}$$

where $\xi$ and $\xi_0$ are the positions of the surface microphone and the "apparent source," measured from the trailing edge, respectively, and $r$ is the distance from the trailing edge to the far-field microphone. Note that the slope, d $(\xi - \xi_0)/d\tau$, of the above equation is given by $U_c$. Further, the equation may be solved to obtain $\xi_0$. When this is done, one finds that the "apparent source" is located slightly upstream of the trailing edge.

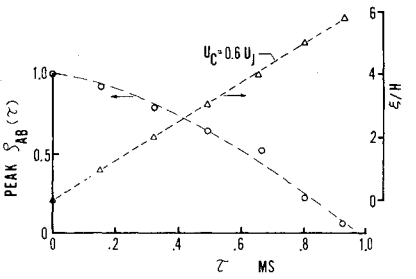


**Fig. 8 Peak correlation of surface pressure and the delay time at which the peak correlation occurs.**

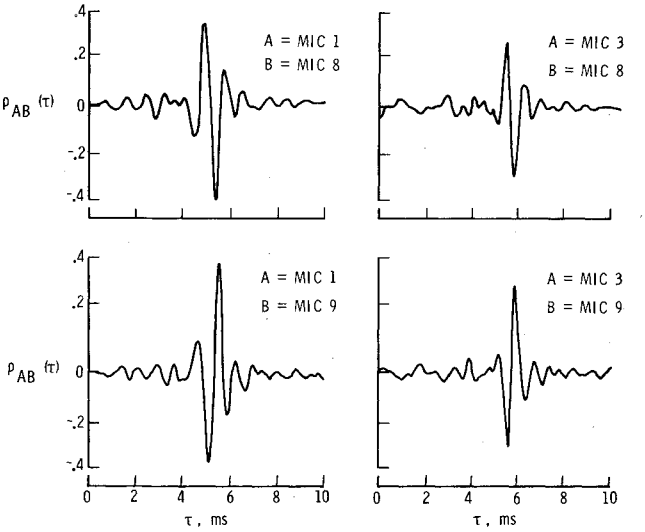


**Fig. 9 Normalized cross-correlation function between surface pressure and far-field noise.**

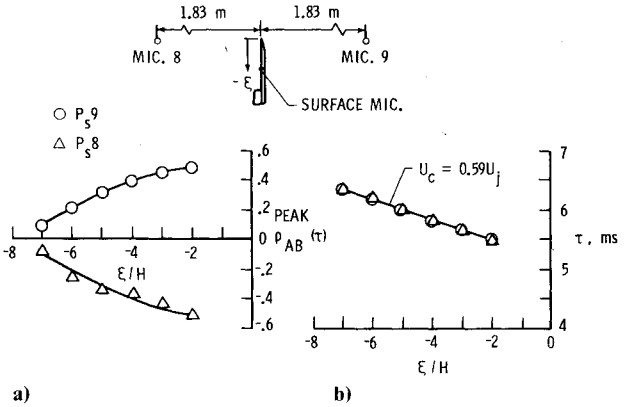


**Fig. 10 Correlation between surface pressure and far-field noise. a) Variation of peak correlation with transducer location and b) variation of delay time for peak correlation.**

Some of the observations regarding the $<p_s p>$ and $<p_s p_s>$ correlations discussediabove have also been reported recently by Fink[13] and Joshi.[14] Fink used an experimental arrangement consisting of a circular nozzle discharging over an airfoil. Joshi's experiment was conducted with a rig similar to the one used in the present experiment, except that both the jet Mach number and nozzle aspect ratio were higher. Although it was deduced in both the investigations of Fink and Joshi that the plate trailing edge was a suspected strong source, the role of the large-scale structure in trailing edge noise generation was not fully recognized. This is the central issue of the following discussions.

### Surface Pressure Fluctuations and Velocity Fluctuations

Consider now the generation of surface pressure fluctuations. Assume that near the flap surface, the flowfield may

be treated as incompressible. Hence, the equation governing the surface pressure is the Poisson equation, with turbulent velocities and mean shear as the source. Thus, it may be possible to deduce the role the large-scale structures play in generating the surface pressure from the correlation of surface pressure and turbulent velocities. Since the transverse motion induced by the large-scale disturbances when coupled with mean shear is believed to be intimately related to both surface pressure and far-field sound, the discussions will concentrate on the correlation between surface pressures $p_s$ and the transverse component of velocity fluctuation $v'$. The spatial correlation $\rho_{p_s v'}(\xi,0)$ obtained between microphone 1 and $v'$ is shown in Fig. 11. In plotting this figure, and also the subsequent figures for the $<pv'>$ correlation, the sign of the correlation obtained directly from the data analysis has been reversed to account for the difference in the transducer response characteristics between hot wire and microphones. Note from Fig. 11 that the $<p_s v'>$ correlation exhibits a characteristic phase reversal at the trailing edge; $<\rho_{p_s v'} > 0$ for the hot wire in the USL and the reverse is true for the hot wire in the TEW. The phase reversal and the characteristic variation of the correlation suggests that the surface pressure near the trailing edge is perhaps generated by two sets of counterrotating vortices,[20] one in the USL and the other with opposite rotation in the TEW. The quasiorderly nature of the structure was again indicated by the oscillations in the spatial correlation.

The variation of the peak correlation and its location in time delay for microphone 1 and the $v'$ fluctuation are given in Fig. 12. Note that the convection speed of the large-scale disturbance is about 0.62 $U_J$ over the flow region of the potential core, in good agreement with the value of 0.6 $U_J$ obtained from the surface-pressure correlation. This is also true in the initial portion of TEW. Further downstream of the trailing edge, however, the apparent convection speed is not constant, but decreases from its initial value of 0.62 $U_J$ to 0.52 $U_J$ at $10H$. This change of apparent $U_c$ is thought to be related to the decrease of the mean velocity downstream from the trailing edge (the potential core ends at $2.5H$ downstream of trailing edge). In addition, the motion induced by the convecting disturbance in the USL and the TEW is in phase opposition, with the $<p_s v'>$ correlation in the USL being negative. The above features are in line with the observations made from $<p_s p_s>$ and $<p_s p>$ correlations.

Figure 12 suggests that, the convected disturbance is correlated with the surface pressure fluctuation in two regions; one near the trailing edge in the upper shear layer and the other at about $3H$ downstream in the trailing edge wake region. Again, if the shadowgraph evidence (see Fig. 3, for example) is used as a guide, it becomes apparent that the two regions of high correlation are actually related to two sets of disturbances. The negative peak on Fig. 12 is related to the convecting large-scale vortices in the upper shear layer. The positive peak is related to large-scale vortices in the trailing edge wake. The location of the correlation peak in the TEW (Fig. 12) coincides approximately with the location of the strong vortex seen from the shadowgraph in the same flow region.

Now compare the results shown on Fig. 12 with those in Fig. 11. Note that the spatial correlation is analogous to observing events simultaneously in space. The space-time cross-correlation following the correlation peaks is analogous to observing events by riding on the convecting disturbance. Figure 11 shows that at any fixed instance, the surface pressure is influenced by the disturbance in the upper shear layer and in the trailing edge wake. Figure 12 also shows that when the disturbances which move at about 0.6 $U_J$ in the upper shear layer are followed, the maximum influence on the surface pressure measured at microphone 1 occurs when the disturbance reaches the trailing edge of the plate. On the other hand, if the disturbance in the trailing edge wake which also moves at about 0.6 $U_J$ initially is followed, the maximum

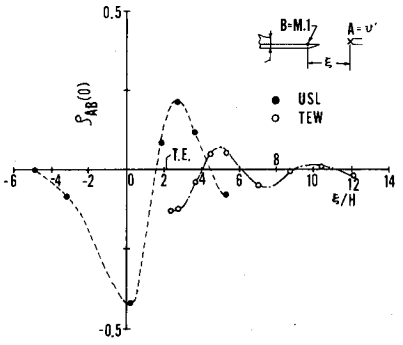


Fig. 11 Spatial correlation between surface pressure and $v'$.

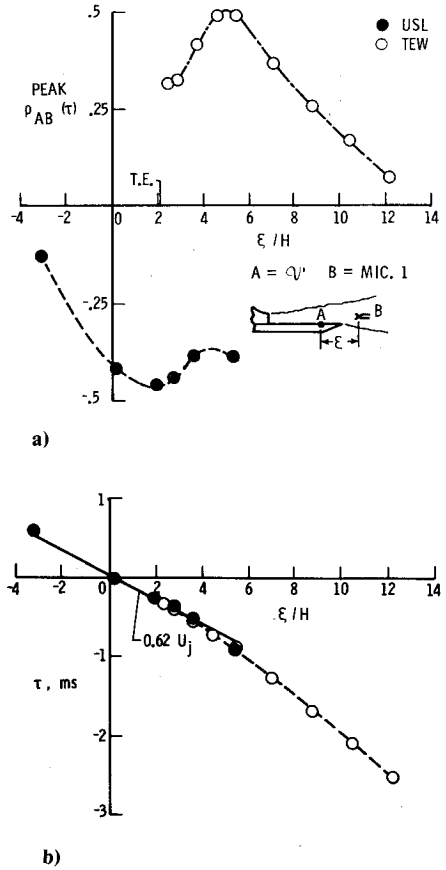


Fig. 12 Correlation between surface pressure and $v'$. a) Variation of peak correlation with hot-wire location and b) variation of delay time for peak correlation.

influence on the surface pressure is reached when the disturbance has traveled about $3.5H$ downstream. These observations collectively suggest that the pressure fluctuation measured on the plate surface is generated by the convection of two families of large-scale vortices both moving at about 0.6 $U_J$ near the trailing edge and having opposite sense of rotation.

### Far-Field Sound and Velocity Fluctuations

The results of $p$ and $v'$ correlations obtained with microphone 8 are shown in Fig. 13. The corresponding results for microphone 9 are almost an exact replica of Fig. 13 except that the signs of the correlation peaks are reversed, hence they are not shown. It is seen that the $<pv'>$ correlations in the upper free shear layer are in phase opposition with those in the TEW. In the USL, the magnitude of the correlation increases nearly monotonically as the hot wire is moved from upstream to downstream of the trailing edge. In the TEW, however, the correlation initially increases from the trailing edge, reaches an extremum at about $3.5H$, then decays. The slope of the $\xi$ vs $\tau$ curve indicates a velocity of 0.61 $U_J$ near

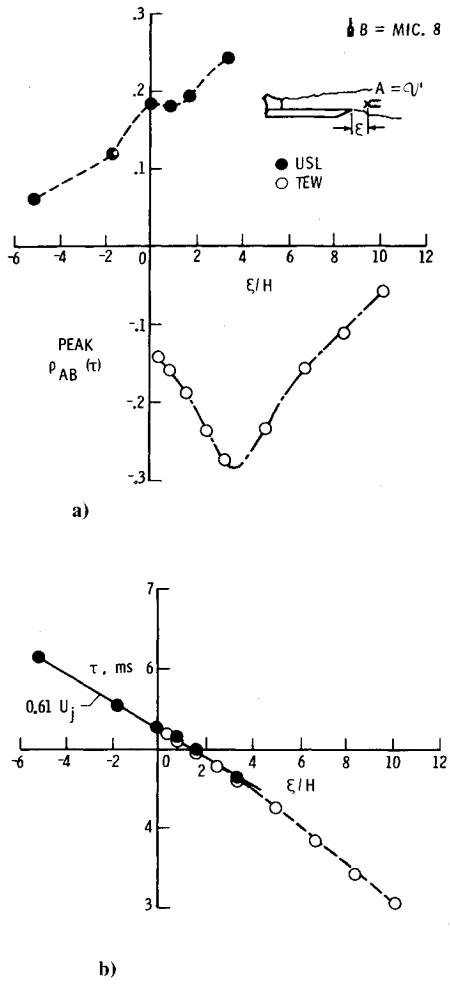


**Fig. 13 Correlation between far-field noise and $v'$. a) Variation of peak correlation with hot-wire location and b) variation of delay time for peak correlation.**

the trailing edge. This value decreases as $v'$ is measured farther downstream of the trailing edge.

The characteristic phase reversal in $<pv'>$ correlations between the USL and the TEW, as has already been observed in the $<p_s v'>$ correlation, relates to the fact that the motion induced by the large-scale structures in the USL is opposite to that in the TEW. Hence, if it is assumed that the far-field sound measured by microphone 8 is in phase with the motion in the USL, it would be antiphase in the TEW. The exact reverse should be true, of course, for microphone 9.

It is tempting to associate the region of flow having comparatively high values of $<pv'>$ correlation with the strong noise source. Thus, one might suspect that the major noise sources for the rather coherent sound field exist at $3.5H$ downstream of the trailing edge. But this is quite misleading as becomes obvious if the time delay associated with the $<pv'>$ correlation in the suspected strong source region is also examined. From Fig. 13 it is seen that the high $<pv'>$ correlation which exits $3.5H$ downstream of the trailing edge actually occurs at a delay time of 4.62 ms. The acoustic transmission time, based on casuality, however, should be 5.27 ms. The large discrepancy between the observed time delay for peak correlation and the acoustic time cannot be accounted for either by the finite bandwidth (10kHz) of the analysis,[21] or by measurement errors in sound speed and path length.

The apparent location of the source can be identified by assuming casuality. The time delay for the $<pv'>$ correlation peak with the hot wire in the USL right above the trailing edge is 5.28 ms, in close agreement with the expected value of 5.27 ms from causality. Thus, the plate trailing edge is a strong suspect. To see if this deduction is compatible with the observed fact that the time delay for peak $<pv'>$ correlation decreases as the hot wire is moved downstream of theitrailing edge, and that the slope of $\xi$ vs $\tau$ c7rve for $<pv'>$ correlation perhaps is related to the convection speed of the large-scale disturbance, it is reasonable to use an analysis similar to that for the $<p_s p>$ correlation. From such an analysis, it can be seen that the slope of $\xi$ vs $\tau$ plot for $<pv'>$ correlation is just the convection speed. This was consistent with the observation made from $<p_s p>$ correlations.

Consider now a possible explanation of the variation of the amplitude of the peaks of $<pv'>$ correlation with wire location. In particular, it would be useful to explain the occurrence of high correlation downstream of the trailing edge. It is argued, that in flow noise problems involving turbulence, the correlation between the cause and consequence may be low, while the correlation between consequences from the same cause can be high. It is possible that the high correlation observed downstream of the trailing edge is a direct result of this. The source of noise and the large-scale vortical structure observed in the TEW, as pointed out earlier, are believed due to the interaction between the upstream large-scale orderly flow structure in the USL and the plate trailing edge. After the interaction (the cause), three things (consequences) can happen: 1) sound may be radiated; 2) the convecting large-scale structure may be modified; and 3) large-scale vortical motion may be induced in the TEW. The correlation obtained between $v'$ measured in the USL near or upstream of the trailing edge with $p$ may thus be a source-consequence correlation. On the other hand, the correlation between $p$ and $v'$ with the hot wire downstream of the trailing edge represents essentially the correlation between consequences from the same cause.

## Discussion of Results

In the previous section, experimental results obtained from flow visualizations and four different types of correlations among various fluctuating field properties are presented. The existence of the large-scale quasiorderly flow structure in the wall jet is indicated by the shadowgraphs (see Figs. 3 and 4) and further supported by the oscillatory nature of the $<p_s p_s>$ and $<p_s v'>$ correlations (see Figs. 7 and 11). The observed flow structure appears to be in the form of convecting vortices (see Figs. 3 and 4). The convection speed is about $0.6U_j$ (see Figs. 8 and 12) with a spatial scale about $4H$ (see Figs. 3, 7, and 11). The sense of rotation of vortices in the USL is apparently opposite to that in the TEW (see Figs. 3, 11-13). The convection of these vortices generates a rather coherent fluctuating surface pressure field (see Figs. 7, 11, and 12).

The role the observed large-scale disturbance plays in generating the coherent sound field (see Fig. 6) was deduced from $<pv'>$ and $<p_s p>$ correlations by invoking a causality assumption. It is found that only over a region in the USL close to the trailing edge, the time delay for peak correlation corresponds to the acoustic transmission time expected from causality (see Figs. 10 and 13). This fact strongly suggests that the physical mechanism of the coherent sound radiation is the interaction between the convecting large-scale quasiorderly flow disturbance in the USL and the trailing edge. The physical process of trailing edge noise production is due to the passage of a quasicoherent field of disturbances over the plate trailing edge. In response to the change of boundary condition imposed at the trailing edge, the convecting disturbances released a rather coherent acoustic radiation. It may be further deduced that the characteristic frequency of radiated sound and surface pressure fluctuation should therefore correspond to the mean passage rate of disturbance over the plate trailing edge. The passage frequency as computed from the convection speed

($0.6U_j$) and the spatial scale ($4H$) is 1500 Hz. This is to be compared with the 1300-Hz common spectral peak measured from far-field sound and surface pressure (see Fig. 5).

It is recognized that different interpretations may be given to the same set of correlation data. The method of interpretation used in analyzing the present correlation results, admittedly not unique, does provide a rather consistent picture of the source field. In fact, deductions made from any one type of correlation are implied and/or enhanced by deductions made from other types of correlation.

The mechanism producing the observed large-scale motion in the upper free shear layer is most probably the flow instability. In this regard, the observed structure is similar to the large-scale structure found in turbulent mixing layers,[17] in two-dimensional jets,[22,23] and in circular jets.[24] The dynamics of formation and development of the observed structure, however, are suspected to be more characteristic of the wall jet flow discharging over a sharp trailing edge.

It is conjectured that the efficiency of this interaction mechanism in the sound production is likely governed by the location of the trailing edge in the wall jet. That is, there could exist a range of edge locations in the wall jet over which the interaction mechanism dominates the sound generation. This range most likely depends on the preferred mode of disturbance in the free shear layer of the wall jet and the amplification achieved by the disturbance when arriving at the trailing edge. It is expected that the acoustic power production by the interaction mechanism should decrease if the trailing edge is located outside this range of the wall jet. In view of the fact that the edge location (or the plate length) is directly involved in the selection of the mode of disturbance for strong interaction, it might also be expected that the frequency of the dominant radiation would scale with the plate length. Experimental evidences in support of the above views have been reported in the literature.[6,14,25,26] It was found that the acoustic power radiation is maximum if the trailing edge terminates near the potential core end of the wall jet[6,14] and the far-field spectrum scales with the plate length.[25,26]

## Concluding Remarks

The highlights of an experimental investigation on the physical mechanism responsible for the generation of trailing edge noise in a turbulent wall jet have been presented. Flow visualization coupled with space-time cross-correlation between the source field and the sound field as used in the present study proved to be very useful in revealing the governing source mechanism. The experimental evidences presented in this paper suggest strongly that the dominant part of the trailing edge noise is generated from the interaction between convecting large-scale quasiorderly disturbances in the free-shear layer of the wall jet and the trailing edge. This interaction produces a highly coherent sound field which is in exact phase opposition across the trailing edge. It also causes the inherently unstable trailing-edge wake to roll up to form large-scale vortices.

## References

[1] Fink, M. R., "Mechanisms of Externally Blown Flap Noise," AIAA Paper 73-1029, Jan. 1973; also, AIAA *Progress in Astronautics and Aeronautics—Aeroacoustics; Fan, STOL, and Boundary Layer Noise; Sonic Boom; Aeroacoustic Instrumentation*, Vol. 38, edited by H. T. Nagamatsu, New York, 1973, pp. 113-128.

[2] Patterson, R. W., Vogt, P. G., Fink, M. R., and Munch, C. L., "Vortex Noise of Isolated Airfoils, *Journal of Aircraft*, Vol. 10, May 1973, pp. 296-302.

[3] Tam, C. K. W., "Discrete Tones of Isolated Airfoils," *Journal of the Acoustical Society of America*, Vol. 55, June 1974, pp. 1173-1177.

[4] Powell, A., "On The Aerodynamic Noise of A Rigid Flat Plate Moving at Zero Incidence," *Journal of the Acoustical Society of America*, Vol. 31, Dec. 1959, pp. 1649-1653.

[5] Ffowcs Williams, J. E., and Hall, L. H., "Aerodynamic Sound Generation by Turbulent Flow in the Vicinity of a Scattering Half Plane," *Journal of Fluid Mechanics*, Vol. 40, March 1970, pp. 657-670.

[6] Hayden, R. E., "Noise from Interaction of Flow with Rigid Surfaces: A Review of Current Status of Prediction Techniques," NASA CR-2126, Oct. 1972.

[7] Chase, D. M., "Sound Radiated by Turbulent Flow Off a Rigid Half-Plane as Obtained from a Wave Vector Spectrum of Hydrodynamic Pressures," *Journal of the Acoustical Society of America*, Vol. 52, Sept. 1972, pp. 1011-1023.

[8] Chase, D. M. "Noise Radiated from an Edge in Turbulent Flow," *AIAA Journal*, Vol. 13, Aug. 1975, pp. 1041-1047.

[9] Chadiramani, K. L. "Diffraction of Evanescent Waves with Applications to Aerodynamically Scattered Sound and Radiation from Unbaffled Plates," *Journal of the Acoustical Society of America*, Vol. 55, Jan. 1974, pp. 19-29.

[10] Amiet, R. K., "Noise Due to Turbulent Flow Past Trailing Edge," *Journal of Sound and Vibration*, Vol. 47, Aug. 1976, pp. 387-393.

[11] Howe, M. S., "A Review of the Theory of Trailing Edge Noise," BBN Rept. 3679, Dec. 1977.

[12] Fink, M. R., "Investigation of Scrubbing and Impingement Noise," NASA CR-134762, Feb. 1975.

[13] Fink, M. R., "Additional Studies of Externally Blown Flap Noise," NASA CR-135096, Aug. 1976.

[14] Joshi, M. C., "Acoustic Investigation of Upper Surface Blown Flaps," Ph.D. Thesis, The University of Tennessee, Knoxville, Tenn., March 1977.

[15] Tam, C. K. W. and Yu, J. C., "Trailing Edge Noise," *Progress in Astronautics and Aeronautics—Aeroacoustics: STOL Noise; Airframe and Airfoil Noise*, Vol. 45, edited by I. R. Schwartz, New York, 1976, pp. 259-280.

[16] Davey, R. F. and Roshko, A., "The Effect of Density Difference on Shear Layer Instability," *Journal of Fluid Mechanics*, Vol. 53, June 1972, pp. 523-543.

[17] Brown, G. L. and Roshko, A. "On Density Effect and Large Structure in Turbulent Mixing Layers," *Journal of Fluid Mechanics*, Vol. 64. July 1974, pp. 775-816.

[18] Lau, J. C., Fisher, M. J., and Fuchs, H. V., "The Intrinsic Structure of Turbulent Jets," *Journal of Sound and Vibration*, Vol. 22, June 1972, pp. 379-406.

[19] Yu, J. C. and Tam, C. K. W., "An Experimental Investigation of Trailing Edge Noise Mechanism," AIAA Paper 77-1291, Oct. 1977.

[20] Blake, W. K. "A Statistical Description of Pressure and Velocity Fields at the Trailing Edges of a Flat Strut," David W. Taylor Ship R&D Center, Bethesda, Md., Rept. 4241, Dec. 1975.

[21] Lee, H. K. and Ribner, H. S., "Direct Correlation of Noise and Flow of a Jet, *Journal of the Acoustical Society of America*, Vol. 52, Nov. 1972, pp. 1280-1290.

[22] Rockwell, D. O. and Niccolls, W. O., "Natural Breakdown of Planar Jets ," *Journal of Basic Engineering*, Vol. 94, Dec. 1972, pp. 720-730.

[23] Rockwell, D. O., "External Excitation of Planar Jets," *Journal of Applied Mechanics*, Vol. 39, Dec. 1972, pp. 883-890.

[24] Crow, S. C. and Champagne, F. H., "Orderly Structure in Jet Turbulence, *Journal of Fluid Mechanics*, Vol. 48, Aug. 1971, pp. 547-591.

[25] Clark, L. R. and Yu, J. C., "Effects of Geometry and Jet Velocity on Noise Associated with an Upper-Surface-Blowing Model," NASA TN D-8386, March 1977.

[26] Reddy, N. N. and Tam, C. K. W., "Analytical Developments for Definition and Prediction of USB Noise," NASA SP-406, May 1976, pp. 241-262.